J. Fluid Mech. (1983), *vol.* 135, *pp.* 175–188
Printed in Great Britain

Viscous thermocapillary convection at high Marangoni number

By STEPHEN J. COWLEY† AND STEPHEN H. DAVIS

Department of Engineering Sciences and Applied Mathematics, The Technological Institute, Northwestern University, Evanston, Illinois 60201

(Received 18 January 1983 and in revised form 3 May 1983)

A liquid, contained in a quarter plane, undergoes steady motion due to thermocapillary forcing on its upper boundary, a free surface separating the liquid from a passive gas. The rigid vertical sidewall has a strip whose temperature is elevated compared with the liquid at infinity. A boundary-layer analysis is performed that is valid for large Marangoni numbers M and Prandtl numbers P. It is found that the Nusselt number N for the horizontal heat transport satisfies $N \sim \min(M^{\frac{2}{7}}, M^{\frac{1}{5}}P^{\frac{1}{16}})$. Generalizations are discussed.

1. Introduction

Motion results whenever a temperature gradient is imposed along the (sufficiently clean) interface between, say, a liquid and a passive gas. This thermocapillary effect is induced from the balance on the interface of the bulk shear stress in the liquid and the surface-tension gradient along the interface. This interfacial stress is transmitted to the bulk by viscous forces.

Forced thermocapillary flows occur in combustion configurations in which a flame propagates over a liquid fuel. Here the large temperature gradient along the fuel surface and the thermocapillary flow generated can dominate the characteristics of the flame by controlling the fuel-mixing properties (see e.g. Sirignano & Glassman 1970; Torrance 1971). Perhaps the simplest such flame-induced motion involves the flow of molten paraffin near the wick of a burning candle (Adler 1970). Clearly, a similar configuration is one involving a spot weld, where a liquid-metal pool is formed by a heat source. Although the material properties of the fluid are different, thermocapillary effects should be involved under similar conditions.

Thermocapillary flows are known to be important in the containerless processing of single crystals. Consider the configuration shown in figure 1 in which a cylindrical solid passes through a heating coil, melts, and then resolidifies into a single crystal. The nature of the crystal formed depends on the local nature of the thermal and fluid-flow fields, so that there is a strong coupling between the fluid dynamics and the growth dynamics of the crystal. Even if the melt consists of a single component, and gravity is absent, there is a thermal-convection field in the melt (as shown), which is driven by variations in the surface tension with the temperature.

Sen & Davis (1982) consider steady Marangoni convection in a rectangular slot that is differentially heated. They use asymptotics for small aspect ratio (thin, flat slots) and obtain representations for the flow and thermal fields. However, their analysis

† Present address: Department of Applied Mathematics and Theoretical Physics, Silver Street, Cambridge CB3 9EW, U.K.

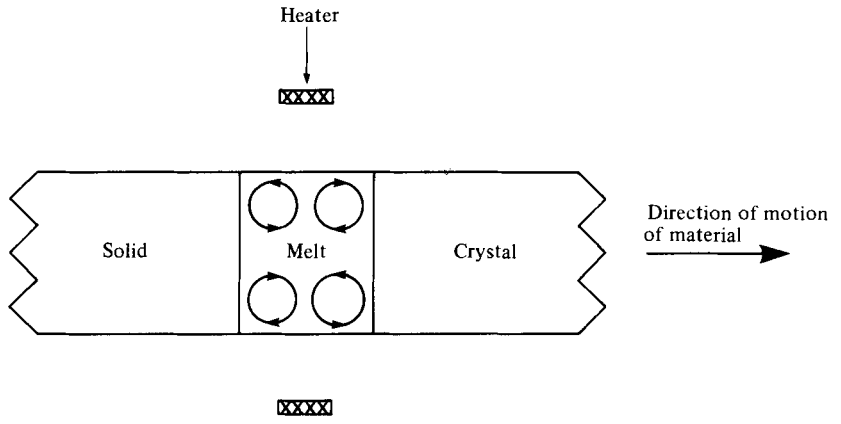

FIGURE 1. Sketch of the geometry of the float-zone crystal-growth process including streamlines of induced thermocapillary convection.

is valid only for small-to-moderate Marangoni numbers M. The flows in the melt of the float-zone process may involve rather large values of M.

We formulate the canonical $M \to \infty$ convection problem. This involves forced steady convection in a quarter-plane. We treat the case where the flow possesses either no viscous boundary layers, or relatively thick ones compared with the thin thermal boundary layers (which convey all the heat). We examine this case, associated with large-Prandtl-number liquids, and obtain estimates for the Nusselt number that measures convective transport parallel to the fluid interface.

There are many similarities between $M \to \infty$ thermocapillary-driven convection in slots and $Ra \to \infty$ buoyancy-driven convection, where Ra is the Rayleigh number. Blythe & Simpkins (1977) review the latter topic. In the present work on the thermocapillary problem we apply a similar approach to that developed by Roberts (1977, 1979) for the buoyancy-driven case. However, we find that in the present problem the scalings and the boundary-layer structures are both quite different from the corresponding buoyancy-driven case. Finally, we discuss generalization to convection in fully enclosed slots.

2. Mathematical formulation

Consider a quarter-plane containing an incompressible Newtonian liquid of density ρ, thermal diffusivity κ and kinematic viscosity ν. Given the Cartesian coordinate system $(\hat{x}, \hat{y})$ shown in figure 2, we define the velocity vector $\hat{\boldsymbol{u}} = (\hat{u}, \hat{v})$ and the pressure $\hat{p}$ and temperature $\hat{T}$.

The upper surface is an interface between the liquid and a passive gas having negligible density, viscosity and thermal conductivity. The wall at $\hat{x} = 0$ is rigid; it is maintained at temperature $\hat{T}_H$ for $-d < \hat{y} < 0$ and it is perfectly insulating for $-\infty < \hat{y} < -d$. The ambient temperature for $\hat{x}^2 + \hat{y}^2 \to \infty$ is given by $\hat{T}_C$. The liquid motion is driven by thermocapillarity on the upper surface. We assume that the surface tension σ depends linearly on $\hat{T}$:

$$\sigma = \sigma_0 - \gamma(\hat{T} - \hat{T}_C). \tag{2.1}$$

We scale the governing system by following, say, Sen & Davis (1982). The length, pressure and temperature scales are respectively d, $\gamma(\hat{T}_H - \hat{T}_C)/d$ and $\hat{T}_H - \hat{T}_C$, and

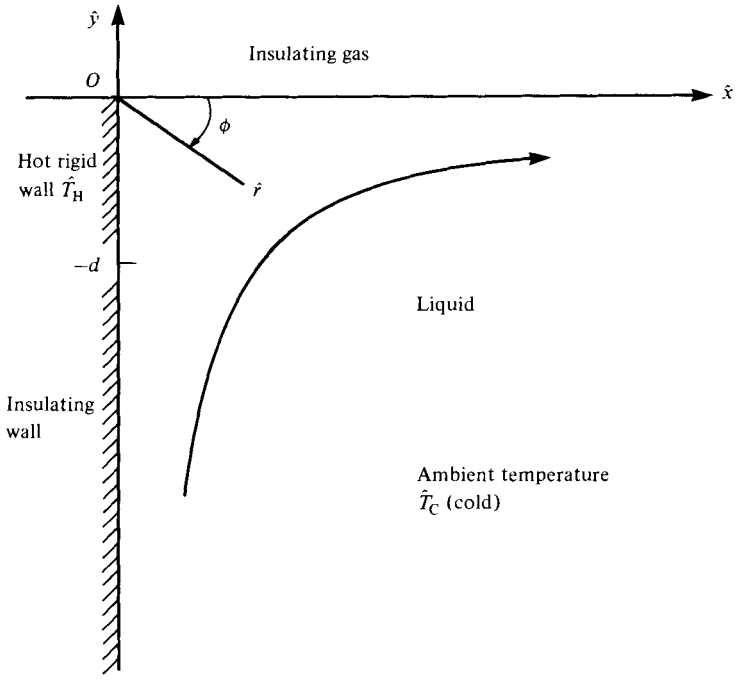

FIGURE 2. Sketch of the quarter-plane region containing the fluid. The planar free surface lies on $\hat{y} = 0$ while the rigid sidewall lies on $\hat{x} = 0$.

we define a Marangoni velocity $u_M = \gamma(\hat{T}_H - \hat{T}_C)/\rho\nu$. Given these scales, the following dimensionless parameters emerge:

the Reynolds number

$$R = \frac{u_M d}{\nu} = \frac{\gamma(\hat{T}_H - \hat{T}_C) d}{\rho\nu^2}, \tag{2.2a}$$

the Marangoni number

$$M = \frac{u_M d}{\kappa} = \frac{\gamma(\hat{T}_H - \hat{T}_C) d}{\rho\nu\kappa}, \tag{2.2b}$$

and the capillary number

$$C = \frac{\rho\nu u_M}{\sigma_0} = \frac{\gamma(\hat{T}_H - \hat{T}_C)}{\sigma_0}. \tag{2.2c}$$

Note that the Prandtl number $P = \nu/\kappa$ is given by

$$P = M/R. \tag{2.2d}$$

We shall assume that $C \to 0$, which implies (Sen & Davis 1982) that the mean surface tension σ_0 is large enough to resist deformation of the upper surface. Thus, the upper surface lies at $\hat{y} = 0$.

If we introduce non-dimensional (caretless) quantities, and measure temperature from $\hat{T}_C$, then the governing equations become

$$R\boldsymbol{u}\cdot\nabla\boldsymbol{u} = -\nabla p + \nabla^2\boldsymbol{u}, \quad \nabla\cdot\boldsymbol{u} = 0, \quad M\boldsymbol{u}\cdot\nabla T = \nabla^2 T. \tag{2.3a,b,c}$$

The associated boundary conditions are

$$u(0,y) = v(0,y) = 0, \tag{2.4a}$$

$$\left.\begin{aligned} T(0,y) &= 1 \quad (-1 < y < 0), \\ T_x(0,y) &= 0 \quad (-\infty < y < -1), \end{aligned}\right\} \tag{2.4b}$$

$$u_y(x,0) + T_x(x,0) = v(x,0) = T_y(x,0) = 0, \tag{2.4c}$$

where we have taken the interface to be a perfect thermal insulator.

We wish to analyse system (2.3)–(2.4) for large values of the Marangoni number. In this case we expect that all variations in liquid temperature will be confined to thin boundary layers of thickness Δ and δ on $x = 0$ and $y = 0$ respectively.

A measure of the heat transport across constant-x sections of the layer is the Nusselt number $N(x)$:

$$N = \int_{-\infty}^{0} (MuT - T_x)\,\mathrm{d}y. \tag{2.5}$$

Since the interface is a perfect insulator, N is x-independent, so that

$$N = -\int_{-\infty}^{0} T_x(0,y)\,\mathrm{d}y. \tag{2.6a}$$

Furthermore, away from the rigid wall, most of the heat flux will occur in the free-surface boundary layer within which streamwise diffusion is negligible. Hence

$$N \sim M\int_{-\infty}^{0} uT\,\mathrm{d}y \quad (x > 0). \tag{2.6b}$$

We can use (2.6a, b) to obtain appropriate scalings for the $M \to \infty$ asymptotic limit. For the moment we assume that inertia and viscous forces are in approximate balance everywhere (so that viscous boundary layers are absent) and there is a single lengthscale governing the viscous flow.†

For large M we denote the magnitude of the core velocity by M^{-b}, and suppose that $\Delta \sim M^{-f}$ and $\delta \sim M^{-d}$. Then, within the thermal boundary layer adjacent to the rigid wall, we have, as a result of the no-slip condition and continuity, that $v \sim \Delta M^{-b} = M^{-b-f}$ and $u \sim \Delta^2 M^{-b} = M^{-b-2f}$; within the surface thermal layer the velocity magnitudes are given by $u \sim M^{-b}$, $u_y \sim M^{-b}$ and $v \sim \delta M^{-b} = M^{-b-d}$. Using these scalings, it follows that, if the advection terms and the dominant diffusion terms of (2.3c) are to balance within both boundary layers, then

$$1 - b = 3f, \quad 1 - b = 2d. \tag{2.7a, b}$$

Furthermore, adjacent to the rigid wall $T \sim 1$, and we suppose that within the surface layer $T \sim M^{-a}$. With these scalings, the thermocapillary boundary condition in (2.4c) yields

$$a = b, \tag{2.7c}$$

while the Nusselt-number condition (2.6) gives

$$1 - a - b - d = f. \tag{2.7d}$$

We solve system (2.7) and obtain the scalings

$$a = b = \tfrac{1}{7}, \quad d = \tfrac{3}{7}, \quad f = \tfrac{2}{7}. \tag{2.7e}$$

† The arguments concerning the single scale are made for reasons of clarity. This restriction will be relaxed later in the text.

If we now return to (2.3*a*), we see that all terms are comparable in the momentum balance in the interior if

$$R \sim M^{\frac{1}{2}} \quad \text{so that} \quad P \sim M^{\frac{6}{7}}. \tag{2.7f}$$

We therefore introduce the scaled Prandtl number

$$\bar{P} = M^{-\frac{6}{7}} P. \tag{2.7g}$$

We note that, because $P \gg 1$, these scalings give different typical surface velocities, say, from those proposed by Ostrach (1982) for $P = O(1)$.

The behaviour of system (2.3)–(2.4) thus reduces to three simplified problems: two boundary problems plus the flow in the isothermal 'core'.

Core flow

In accordance with scalings (2.7*e*) we define the velocity field

$$(u, v) = M^{-\frac{1}{7}}(\psi_{0y}, -\psi_{0x}) + \ldots, \tag{2.8}$$

where the stream function ψ_0 is negative. We shall see below that all thermal variations are negligibly small, so that the core solution to the heat equation (2.3*c*) is zero. The equation of motion (2.3*a*) becomes

$$\psi_{0y}\omega_{0x} - \psi_{0x}\omega_{0y} = \bar{P}\nabla^2\omega_0, \tag{2.9a}$$

where

$$\omega_0 = -\nabla^2\psi_0. \tag{2.9b}$$

The rigid-wall boundary conditions on $x = 0$, and the kinematic boundary condition on $y = 0$, become

$$\psi_0 = \psi_{0x} = 0 \quad (x = 0), \quad \psi_0 = 0 \quad (y = 0). \tag{2.9c}$$

The final boundary condition is the Marangoni condition (2.4*c*) on the free surface. This will be given in simplified form after solutions within the thin thermal boundary layers have been found.

Boundary layer on the rigid wall

We use the scalings (2.7*e*), write

$$x = M^{-\frac{2}{7}}X, \quad T = T_0 + \ldots, \tag{2.10}$$

and note that the no-slip boundary condition implies that $\psi_0 \sim \frac{1}{2}x^2\psi_{0xx}(0, y)$. If we substitute into the heat equation (2.3*c*) and the thermal boundary conditions, we obtain

$$\tfrac{1}{2}X^2\psi_{0xxy}(0, y)\, T_{0X} - X\psi_{0xx}(0, y)\, T_{0y} = T_{0XX}, \tag{2.11a}$$

$$T_0(0, y) = 1 \quad (-1 < y < 0), \quad T_{0X}(0, y) = 0 \quad (-\infty < y < -1). \tag{2.11b}$$

By means of a transformation used by Lighthill (1950) and Acrivos & Goddard (1966), Roberts (1977) has found the solution to (2.11) which decays as $X \to \infty$:

$$T_0 = \begin{cases} [\Gamma(\frac{1}{3})]^{-1} \displaystyle\int_\zeta^\infty \xi^{-\frac{2}{3}} e^{-\xi}\, \mathrm{d}\xi & (-1 < y < 0), \\ 0 & (-\infty < y < -1), \end{cases} \tag{2.12a}$$

where

$$9s\zeta = 4n^{\frac{3}{2}}, \quad n = -\tfrac{1}{2}X^2\psi_{0xx}(0, y), \quad s(y) = \int_{-1}^{y} [-2\psi_{0xx}(0, y)]^{\frac{1}{2}}\, \mathrm{d}y. \tag{2.12b}$$

The scaled Nusselt number

$$\bar{N} \equiv NM^{-\frac{2}{7}} \tag{2.13a}$$

is therefore given by

$$\bar{N} = (\tfrac{3}{2})^{\frac{4}{3}} \frac{[s(0)]^{\frac{8}{3}}}{\Gamma(\frac{1}{3})}. \tag{2.13b}$$

Boundary layer on the free surface

The scalings (2.7*e*) suggest the expansions

$$y = M^{-\frac{3}{7}} Y, \quad T = M^{-\frac{1}{7}} \bar{T}_0 + \ldots. \tag{2.14a, b}$$

The condition of zero crossflow through the free surface gives that $\psi_0 \sim y\psi_{0y}(x, 0)$. If we substitute forms (2.14) into the heat equation (2.3*c*) and the free-surface conditions (2.4*c*), we find that

$$\psi_{0y}(x, 0)\, \bar{T}_{0x} - Y\psi_{0xy}(x, 0)\, \bar{T}_{0Y} = \bar{T}_{0YY}, \tag{2.15a}$$

with

$$\bar{T}_{0Y} = 0 \quad (Y = 0), \quad \bar{T}_0 \to 0 \quad (Y \to \infty). \tag{2.15b}$$

In order for system (2.15) to be well-posed, a further condition is needed at $x = 0$. This condition is found by examining the heat balance nearer the corner, although there is no need to explicitly solve the problem in the corner. As will be explained in greater detail in §3, as the flow enters the corner, heat is effectively only being convected along streamlines (since diffusion is negligible). However, as a result of the change from rigid to free-surface boundary conditions, the streamlines move closer together and eventually diffusion becomes important in a region adjoining the free surface and close to the corner. Far downstream from this 'diffusion' region, the details of the solution within this region are unimportant, and the flow effectively sees only a source of heat of magnitude $\bar{N}$. The required solution to system (2.15) is therefore as given by Roberts (1977):

$$\bar{T}_0 = \frac{\bar{N}}{(\pi S)^{\frac{1}{2}}} \exp\left[-\frac{\psi_{0y}^2(x, 0)\, Y^2}{4S}\right], \tag{2.16a}$$

where

$$S = \int_0^x \psi_{0y}(x, 0)\, \mathrm{d}x. \tag{2.16b}$$

Using (2.16), the Marangoni balance of (2.4*c*) can be transformed to obtain the final boundary condition to (2.9):

$$2(\pi S^3)^{\frac{1}{2}} \psi_{0yy}(x, 0) = \bar{N}\psi_{0y}(x, 0). \tag{2.17}$$

Reduced Navier–Stokes problem

Equations (2.9*a*, *b*) and boundary conditions (2.9*c*) and (2.17) specify a Navier–Stokes problem in which all the parameters can be scaled out. A parameter is reintroduced only when (2.13) is used to solve for $\bar{N}$. Following a suggestion of a referee, we therefore scale $\bar{N}$ and $\bar{P}$ from (2.9) and (2.17) by writing

$$\psi_0 = \bar{P}\tilde{\psi}, \quad (x, y) = L(\tilde{x}, \tilde{y}), \tag{2.18}$$

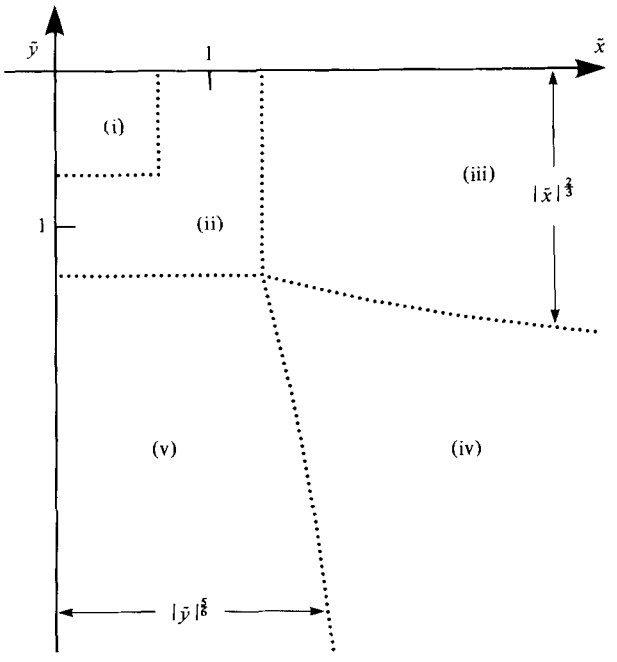

FIGURE 3. Regions of the solution to (2.19): (i) Stokes flow; (ii) region where all terms in (2.19*a*) balance; (iii) surface viscous boundary layer; (iv) inviscid core; (v) 'backwards' viscous boundary layer (see §4).

where $L = \bar{P}^{\frac{1}{3}}\bar{N}^{-1}$. Equations (2.9), (2.12*b*), (2.13*b*), (2.16*b*) and (2.17) then become

$$\tilde{\psi}_{\tilde{y}}\tilde{\omega}_{\tilde{x}} - \tilde{\psi}_{\tilde{x}}\tilde{\omega}_{\tilde{y}} = \tilde{\nabla}^2\tilde{\omega}, \quad \tilde{\omega} = -\tilde{\nabla}^2\tilde{\psi}; \tag{2.19a}$$

$$\tilde{\psi} = \tilde{\psi}_{\tilde{x}} = 0 \quad (\tilde{x} = 0); \quad \tilde{\psi} = 0, \quad 2(\pi S^3)^{\frac{1}{2}}\tilde{\psi}_{0\tilde{y}\tilde{y}} = \tilde{\psi}_{0\tilde{y}} \quad (\tilde{y} = 0); \tag{2.19b}$$

$$\bar{S} = \int_0^{\tilde{x}} \tilde{\psi}_{\tilde{y}}(\tilde{x}, 0)\,\mathrm{d}\tilde{x}; \quad 4[\Gamma(\tfrac{1}{3})\bar{N}]^{\frac{3}{2}} = 9\bar{P}^{\frac{1}{2}}\int_{-1/L}^{0} [-2\tilde{\psi}_{\tilde{x}\tilde{x}}(0, \tilde{y})]^{\frac{1}{2}}\,\mathrm{d}\tilde{y}. \tag{2.19c,d}$$

Different regions of the solution to (2.19*a–c*) can be identified by noting that $\tilde{r} = (\tilde{x}^2 + \tilde{y}^2)^{\frac{1}{2}}$ can be viewed as a local Reynolds number of the flow. Where $\tilde{r} = O(1)$ all terms in the governing equations are of equal importance and a numerical solution is required. However, analytical progress should be possible for $\tilde{r} \ll 1$ and $\tilde{r} \gg 1$. Near the corner a Stokes-flow region will exist, while far from the corner the flow will consist of an inviscid core and viscous boundary layers (see figure 3). We also note from (2.19*d*) that, in the limit $L \to \infty$ (i.e. $\bar{P} \to \infty$), it should be possible to determine $\bar{N}$ by solving only in the Stokes-flow regime. Conversely, for $L \to 0$ (i.e. $\bar{P} \to 0$), we might expect to determine $\bar{N}$ by just examining the far-field regime.

In the next two sections we consider the Stokes flow and far-field regimes in turn. Particular reference will be given to the limits $\bar{P} \to \infty$ and $\bar{P} \to 0$.

3. Stokes-flow region

For $\tilde{r} \ll 1$ (2.19*a*) simplifies to

$$\tilde{\nabla}^4\tilde{\psi} = 0. \tag{3.1}$$

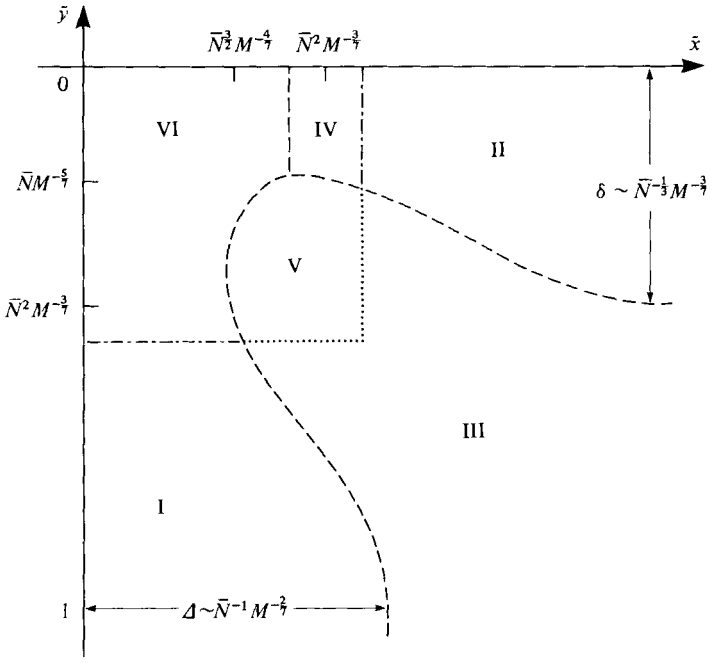

FIGURE 4. Schematic of the asymptotic for $\bar{P} = O(1)$: ---, boundaries of thermal regions; · · ·, boundaries of viscous regions; I, II, IV and VI are thermal regions, III and V are viscous regions.

The boundary conditions (2.19*b*, *c*) suggest seeking solutions of the form $\tilde{\psi} = \tilde{r}^m f(\phi)$, where $\tan\phi = -\tilde{y}/\tilde{x}$. The solution is

$$\tilde{\psi} = \frac{1}{6}\left(\frac{\tilde{r}^2}{10\pi}\right)^{\frac{1}{3}} [3\sqrt{3}\cos\tfrac{2}{3}\phi - 7\sin\tfrac{2}{3}\phi - 3\sqrt{3}\cos\tfrac{4}{3}\phi + \sin\tfrac{4}{3}\phi]. \tag{3.2}$$

If $\bar{P} \gg 1$ then the integral in (2.19*d*) can be evaluated asymptotically using (3.2) to obtain

$$\bar{N} = 3^{\frac{27}{14}}(80\pi)^{-\frac{1}{7}}[\Gamma(\tfrac{1}{3})]^{-\frac{9}{7}} \approx 1.06. \tag{3.3a}$$

Hence for $\bar{P} \gg 1$ the behaviour of Nusselt number with Marangoni number is

$$N \sim 1.06 M^{\frac{3}{7}}. \tag{3.3b}$$

The most striking physical behaviour of the solution (3.2) is the increase of fluid speed as one approaches the corner along the free surface. This is in contrast with the analogous Bénard problem, studied by Roberts (1977), for which the fluid speed falls as one approaches the corner. Further, despite this increase in fluid speed, the ratio of viscous forces to inertial forces increases. Hence the present scaling breaks down closer to the corner not because of inertial effects, but because of inadequacies in the description of the temperature distribution. The resulting asymptotic regions are illustrated in figure 4.

Region IV is the 'diffusion' region mentioned in §2. Since we have hypothesized that heat is *convected* in region VI (i.e. the region where the temperature is non-zero near the corner), it follows that $T \sim 1$ in region IV. The size of this region can now be deduced from (2.16) and (3.2), for we see that $\bar{T}_0 \sim M^{\frac{1}{7}}$ when $x \sim \bar{N}^2 M^{-\frac{3}{7}}$ and $y = M^{-\frac{3}{7}}Y \sim \bar{N}M^{-\frac{4}{7}}$. So in region V ($x \sim y \sim \bar{N}^2 M^{-\frac{3}{7}}$) the stream function is no longer given by (3.2) to leading order because modifications are necessary to the Marangoni boundary condition (2.17).

The mathematical problems to be solved in regions IV and V are straightforward

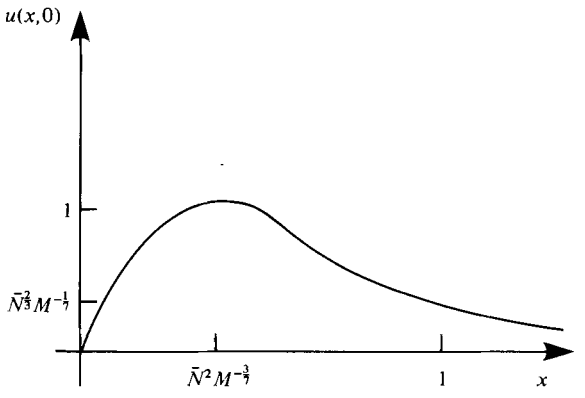

FIGURE 5. Sketch of the surface speed.

to formulate. In region IV it again proves necessary to solve the thermal boundary-layer system (2.15). However, whereas in region II $x = 0$ can be regarded as a point source, in region IV the temperature profile at $x = 0$ needs to be related to that at $y = 0$ in the rigid-wall boundary layer (region I). Because heat is convected along streamlines in region VI, this matching is easily achieved by introducing streamline coordinates (Roberts 1977; Kuiken 1978). Roberts (1977) gives an analytical solution to the resulting problem. Using this solution, the Marangoni surface condition for region V can be deduced from (2.4*c*). The Stokes-flow problem for region V so formulated requires a numerical solution. Although we have not found this solution, we note that it is in region V that the maximum velocities are attained. A graph of the surface velocity u_s therefore looks as illustrated in figure 5. We conclude from (2.8), (2.18), (3.2) and the dimensions of region V that $\max(u_s) = O(1)$ for all non-zero $\bar{P}$.

The shape of region VI can be deduced as follows. First, from (2.12), (2.13) and (3.2) we conclude that $\Delta \sim \bar{N}^{\frac{2}{7}}M^{-\frac{1}{7}}$ when $|y| \sim \bar{N}^{2}M^{-\frac{3}{7}}$, and that $\psi \sim \bar{N}M^{-\frac{1}{7}}$ within region VI. Hence the temperature excess is confined to a region close to the wall. Further, when $|x|, |y| \ll \bar{N}^{2}M^{-\frac{3}{7}}$, $\psi \sim$ (constant) $\bar{N}^{-4}M^{\frac{1}{7}}x^{2}y$ (where ψ is the non-scaled stream function), and it can be confirmed *a posteriori* that heat is convected and not conducted in region VI. Therefore $\Delta \sim \bar{N}^{\frac{2}{7}}|y|^{-\frac{1}{2}}M^{-\frac{11}{14}}$ (or equivalently $\delta \sim \bar{N}^{5}x^{-2}M^{-\frac{11}{7}}$) when $|x|, |y| \ll \bar{N}^{2}M^{-\frac{3}{7}}$. We note that this suggests $\delta \sim NM^{-\frac{5}{7}}$ when $x \sim N^{2}M^{-\frac{3}{7}}$, which is in agreement with the scaling proposed for region IV. Our scalings would hence appear to be self-consistent.

4. Far-field solution

For $\tilde{r} \gg 1$ the local Reynolds number is large. Thin viscous boundary layers are therefore expected to develop adjacent to the surfaces. By analogy with the solution for a buoyant plume (Kuiken & Rotem 1971), we begin by seeking a similarity solution for the viscous boundary layer on the free surface. Expanding in inverse powers of $\tilde{x}$, we let

$$\tilde{\psi} \sim \tilde{x}^{\frac{1}{4}}f(\eta), \quad \eta = \tilde{y}\tilde{x}^{-\frac{3}{4}}, \tag{4.1}$$

and substitute into (2.19*a–c*); we obtain

$$4f''' + ff'' + 2f'^{2} = 0, \tag{4.2a}$$

$$f(0) = f'(-\infty) = 0, \quad 4[2\pi f'(0)]^{\frac{1}{2}}f''(0) = 1. \tag{4.2b}$$

If we integrate (4.2a) once, and use conditions (4.2b), we find that

$$+[2\pi f'(0)]^{\frac{1}{2}}\int_{-\infty}^{0} f'^2\,\mathrm{d}\eta = -1. \tag{4.3}$$

This is impossible, and hence there is no similarity solution of this form. The physical reason for this appears to be that the deceleration of the surface fluid required by the Marangoni condition is larger than the deceleration that can be forced on the interior fluid (with its accompanying inertia). Under such circumstances an interior maximum of the velocity profile would normally form, implying that $u_{\tilde{y}}(\tilde{x},0)<0$. This is unlikely, as it implies through (2.4c) that the temperature increases away from the wall!

It is possible to resolve the above difficulty by assuming that the surface-tension distribution where $\tilde{r}=O(1)$ establishes a surface jet in $\tilde{x}\gg 1$ which is too strong to be influenced to leading order by the surface-tension distribution there. So, for $\tilde{x}\gg 1$, the leading-order solution is a jet with $u_{\tilde{y}}(\tilde{x},0)=0$, and with magnitude determined by the $\tilde{r}=O(1)$ region.

A surface similarity solution of the following form is therefore sought:

$$\tilde{\psi} = \tilde{x}^{\frac{1}{3}}[f_0(\eta)+\tilde{x}^{-\frac{1}{3}}f_1(\eta)+\ldots], \quad \eta=\tilde{y}\tilde{x}^{-\frac{2}{3}}. \tag{4.4}$$

The powers of $\tilde{x}$ are chosen to recover the classical 'jet' similarity solution (see Batchelor 1967) to leading order. The resulting governing equations are

$$f_0'''=-\tfrac{1}{3}f_0f_0''-\tfrac{1}{3}f_0'^2, \quad f_1'''=-\tfrac{1}{3}f_0f_1''-f_0'f_1', \tag{4.5a,b}$$

together with the boundary conditions

$$f_0(0)=f_0''(0)=f_0'(-\infty)=0, \tag{4.6a}$$

$$f_1(0)=0, \quad [\tfrac{27}{2}\pi f_0'(0)]^{\frac{1}{2}}f_1''(0)=1. \tag{4.6b}$$

The final boundary condition on f_1 comes from matching with the inviscid core. The solution for f_0 is

$$f_0 = 6k\tanh k\eta. \tag{4.7}$$

Because the leading-order solution is an eigenfunction, the constant k can only be fixed by solving the full system of equations (2.19a–c) for $\tilde{r}=O(1)$. This situation is analogous to that for flow over a blunt-nosed semi-infinite flat plate where the coefficients of the eigenfunctions can only be determined by finding the solution in a 'Navier–Stokes' region near the leading edge. It is unlike the equivalent buoyancy problem, for which the leading-order solution for $\tilde{r}\gg 1$ is fully determined.

Within the inviscid core we set $\tilde{\psi}\sim\bar{\Psi}$. Then $\tilde{\nabla}^2\bar{\Psi}(\tilde{x},\tilde{y})=\bar{\Psi}_{\tilde{y}}(0,\tilde{y})=0$, and, from matching with form (4.4) and (4.7), $\bar{\Psi}(\tilde{x},0)=-6k\tilde{x}^{\frac{1}{3}}$. Therefore $\bar{\Psi}$ has the solution

$$\bar{\Psi} = -12k\tilde{r}^{\frac{1}{3}}\sin(\tfrac{1}{6}\pi-\tfrac{1}{3}\phi). \tag{4.8}$$

The remaining boundary condition for f_1 is consequently $f_1'(-\infty)=-2\sqrt{3}\,k$, and hence

$$f_1 = (18k^3)^{-1}\pi^{-\frac{1}{2}}\tanh^2 k\eta+3\sqrt{3}\tanh k\eta-\sqrt{3}\,k\eta(2-3\,\mathrm{sech}^2 k\eta). \tag{4.9}$$

The inviscid slip velocity induced by $\bar{\Psi}$ along the rigid wall is $4k(-\tilde{y})^{-\frac{2}{3}}$. This generates a boundary layer, for which the appropriate scalings are

$$\tilde{\psi}\sim 2k^{\frac{1}{2}}(-\tilde{y})^{\frac{1}{3}}g(\zeta), \quad \zeta=2k^{\frac{1}{2}}\tilde{x}(-\tilde{y})^{-\frac{2}{3}}. \tag{4.10}$$

The governing equations and boundary conditions are those for the so-called 'backward boundary layer' (Goldstein 1965):

$$6g''' + gg'' + 4(g'^2 - 1) = 0, \tag{4.11a}$$

$$g(0) = g'(0) = 0, \quad g'(\infty) = -1. \tag{4.11b}$$

A numerical solution, with $g''(0) = -0.9279$, can be found to this system of equations.

For all non-zero $\bar{P}$ it is therefore possible to find a consistent asymptotic expansion valid for $\tilde{r} \gg 1$. If $\bar{P} \ll 1$, then the main contribution to the integral in (2.19*d*) comes from this far-field region. Substitution of (4.10) into (2.19*d*) then yields

$$\bar{N}^{\frac{4}{3}} \sim 6[-6g''(0)]^{\frac{1}{3}} k^{\frac{1}{3}} [\Gamma(\tfrac{1}{3})]^{-1} \bar{P}^{\frac{1}{12}}. \tag{4.12}$$

When (4.12) is combined with definition (2.13*a*) and the above numerical value of $g''(0)$, we find that

$$N \sim 5.23 k^{\frac{1}{3}} \bar{P}^{\frac{1}{10}} M^{\frac{4}{3}}. \tag{4.13}$$

This asymptotic expansion is valid for $M^{-\frac{4}{3}} \ll \bar{P} \ll 1$, i.e. $1 \ll P \ll M^{\frac{4}{3}}$. The lower limit, $P \sim 1$, corresponds to the thermal and viscous boundary layers being of comparable thicknesses. It would be necessary to solve (2.19*a–c*) numerically in order to determine k. We do not attempt this here.

5. Discussion and conclusions

We have considered liquid lying in the quarter-plane $x > 0$, $y < 0$. The solid boundary at $x = 0$ is insulated for $y < -1$ and held at a fixed unit temperature for $-1 < y < 0$. The boundary $y = 0$ is a non-deflecting thermally insulated interface on which thermocapillary forces exist. The temperature far from the origin is zero.

We have assumed steady thermocapillary flow for large Marangoni numbers M. We assume that thin thermal boundary layers exist on the solid and free surfaces, and that the core flow is isothermal. Further, the Prandtl number P is assumed sufficiently large so that the thermal layers are of prime importance; i.e. the parameter regimes studied either have no viscous boundary layers or have viscous boundary layers that are much thicker than the thermal layers.

Within the thermal boundary layers tangential convection balances normal conduction. The vertical sidewall layer has thickness $M^{-\frac{3}{4}}$ and temperature order unity; the horizontal free-surface layer has thickness $M^{-\frac{3}{4}}$ and temperature order $M^{-\frac{1}{4}}$. By introducing a scaled Prandtl number $\bar{P} = M^{-\frac{1}{4}}P$, and expanding in inverse powers of M, the coupled thermoconvection problem is reduced to solving the Navier–Stokes equations with novel boundary conditions. For all $\bar{P}$ the velocity field can be separated into (i) a Stokes-flow region, (ii) a region where all the terms in the Navier–Stokes equation are of equal importance, and (iii) a far-field region constituting of an inviscid core surrounded by viscous boundary layer. For $\bar{P} = O(1)$ numerical methods are required. However, if $\bar{P}$ is large, then the heated strip falls totally within the Stokes-flow region, and we find that

$$N \sim 1.06 M^{\frac{4}{3}}, \quad \bar{P} \gg 1. \tag{5.1a}$$

Conversely, if $\bar{P}$ is small, then the magnitude of the heated strip is adjacent to a viscous boundary layer, and

$$N \sim 5.23 k^{\frac{1}{3}} \bar{P}^{\frac{1}{10}} M^{\frac{4}{3}}, \quad M^{-\frac{4}{3}} \ll \bar{P} \ll 1. \tag{5.1b}$$

Here k is an undetermined constant associated with an 'eigenfunction' solution of the free-surface viscous boundary layer.

The assumption that the liquid–gas interface is non-deformable is valid in the limit of capillary number $C = M\rho\nu\kappa/\sigma_0 d \to 0$. If the free surface is given by $y = h(x)$, then for $\bar{P} \sim 1$ the simplified free-surface boundary conditions (2.4c), which result from this assumption, are correct if $|h| \ll M^{-\frac{3}{7}}$. However, for $M^{-\frac{3}{7}} \lesssim |h| \ll 1$, the free-surface boundary conditions must be modified to

$$u_y + T_x + h_x T_y = v - uh_x = T_y = 0 \quad (y = h). \tag{5.2}$$

The core-flow problem specified by (2.19) is nevertheless correct for $|h| \ll 1$. This may be demonstrated by introducing the Prandtl transformation

$$y = h(x) + M^{-\frac{3}{7}} Y \tag{5.3}$$

in place of (2.14a). The substitution of the condition $|h| \ll 1$ into the full free-surface boundary conditions (Sen & Davis 1982) results in the restriction $\rho\nu\kappa/\sigma_0 d \ll M^{-\frac{4}{7}}$. Typically, the group $\rho\nu\kappa/\sigma_0 d$ lies in the range 10^{-5}–10^{-3}, so that, even for reasonably large values of M, surface deflections can be ignored.

We have also taken the liquid–gas interface to be a perfect thermal insulator. In actuality some heat is lost to the gas; convective transport in the gas leads to a generalized thermal boundary condition of the form $T_y + BT = 0$ on $y = 0$, where B is a surface Biot number. For $\bar{P} \sim 1$ the present analysis remains correct if B lies in the range $B \ll M^{\frac{3}{7}}$. If $B \gg M^{\frac{3}{7}}$, the problem decouples, and given the temperature of the gas it is possible to solve for the velocity and temperature fields consecutively.

We note that variations of surface tension with temperature are often accompanied by significant variations in viscosity. Furthermore, if phase changes (solidification) occur, complex rheological behaviour may be important. The inclusion of such effects is left for further study.

The solution we have found is the thermocapillary analogue of buoyancy-driven convection in a quarter-plane as described by Roberts (1977). The approach and the methods used are similar. However, the scalings, physical balances and details are different. For example:

(i) The surface velocity decreases monotonically to zero towards the corner in the buoyancy case, while it has a maximum in the thermocapillary case. For all $\bar{P}$ the maximum is achieved in region IV where $x = O(\bar{N}^2 M^{-\frac{3}{7}})$, and $\max(u(x, 0)) = O(1)$. From (3.3a) and (4.12) it follows that, as $\bar{P}$ decreases, this maximum moves closer to the corner.

(ii) The velocity field solution to region III is no longer valid in region IV in the thermocapillary case, whereas it remains valid in the equivalent 'diffusion' region for the buoyancy problem.

(iii) Unlike the thermocapillary problem there is no undetermined constant in the leading-order expansion of the far-field solution for the buoyancy problem.

These differences are attributable to the differences in the driving forces: a surface-concentrated force depending on the details of the thermal boundary layer in the former problem, compared with a body force depending on an integral across the thermal boundary layer in the latter.†

† If the rigid boundary at $x = 0$ is replaced by a stress-free plane, then the relation (2.7a) of §2 is replaced by $1 - b = 2f$, giving $a = b = 0$, $d = f = \frac{1}{2}$ and $N = O(M^{\frac{1}{7}})$. Unlike the analogous buoyancy-driven stress-free case (Roberts 1977) the solutions in the present thermocapillary case depend on the details of the thermal boundary layer and not on a quantity obtained from integrating across the layer. Hence numerical solutions of the governing equations are required. We do not pursue this case further since it is not directly relevant to the applications discussed in §1.

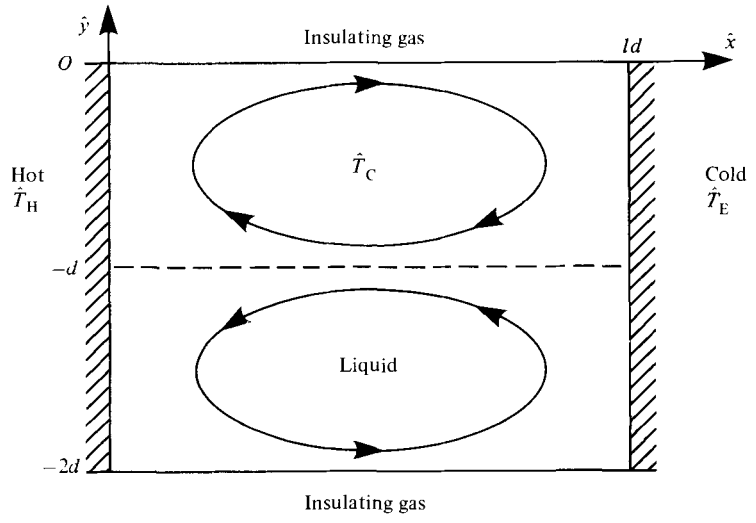

FIGURE 6. An example slot flow; $\hat{y} = -d$ is a line of symmetry.

The highly simplified model described herein has been considered because for $\bar{P} = O(1)$ it is expected to incorporate the dominant balances associated with large-Marangoni-number convection in slots of approximately unit aspect ratio. For instance, the scaling arguments of §2 carry through for the slot illustrated in figure 6. $\hat{T}_H$ is again the temperature of the hot wall, while $\hat{T}_C$ is now the temperature of the central core region. Because $\hat{T}_C$ is used as the reference temperature, the temperature $\hat{T}_E$ of the cold wall is part of the solution of the problem. $\hat{T}_E$ is fixed by requiring that the heat flux at the cold wall equals that at the hot wall. The governing equations of the flow in $-1 \leqslant y \leqslant 0$ are again (2.9*a*, *b*). The boundary conditions are (2.9*c*), (2.16*b*), (2.17) and

$$\psi_0 = \psi_{0x} = 0 \quad (x = l), \quad \psi_0 = \psi_{0yy} = 0 \quad (y = -1). \tag{5.4}$$

Although a numerical solution is necessary for all $\bar{P}$, we note that the most vigorous thermocapillary convection will again be confined to very small corner regions. As far as crystal-growing configurations are concerned, this suggests that the worst convection-generated defects can be anticipated to occur near the corners.

For $\bar{P} \gg 1$, Stokes flow fills the whole slot, and the analysis of §3 can easily be adapted to show that $\bar{N}$ tends to a constant as $\bar{P} \to \infty$. However, in the limit $\bar{P} \to 0$, the structure of the slot-flow solution is likely to differ significantly from the solution proposed in §4 for the quarter-plane. In particular, the inviscid core flow is likely to be rotational and have velocity magnitudes comparable to those in the free surface boundary layers. If so, the possibility arises that an adverse pressure gradient will develop adjacent to one of the rigid boundaries, so leading to separation (see Wesseling's (1969) comments on an analogous buoyancy problem). Nevertheless, the structure of the solution in §4 could be of relevance to a 'start-up' slot problem, as it may be correct for a quasi-steady solution valid some time after the initial transients have died out, but before vorticity has fully diffused throughout the core. The work of §4 is also of interest as an example of a 'backwards' boundary layer, in non-quiescent irrotational surroundings, extending over a finite length of wall (see Kuiken 1981*a*, *b*).

Finally, we note that we have examined only the two-dimensional quarter-plane idealization consistent with the analysis of Marangoni convection in a

two-dimensional slot. The application of large-Marangoni-number convection to crystal growth involves flow and heat transfer in a *circular cylinder*. The extension of the scale analysis to this case is straightforward. However, *inter alia* the details of the boundary-layer solution on the rigid walls would change.

This work was funded by the National Aeronautics and Space Administration, Materials-Processing-in-Space-Program and Fitzwilliam College, Cambridge. The referees are thanked for their helpful suggestions. S.J.C. is grateful to Dr M. R. E. Proctor for a useful discussion.

REFERENCES

ACRIVOS, A. & GODDARD, J. D. 1965 Asymptotic expansions for laminar forced-convection heat and mass transfer. Part 1. Low speed flows. *J. Fluid Mech.* **23**, 273.

ADLER, J. 1970 Fluid mechanics of a shallow fuel layer near a burning wick. *Combust. Sci. Tech.* **2**, 105.

BATCHELOR, G. K. 1967 *An Introduction to Fluid Dynamics*. Cambridge University Press.

BLYTHE, P. A. & SIMPKINS, P. G. 1977 Thermal convection in a rectangular cavity. In *Proc. Intl Symp. Physico-Chem. Hydrodyn., Oxford, England.*

GOLDSTEIN, S. 1965 On backward boundary layers and flow in converging passages. *J. Fluid Mech.* **21**, 33.

KUIKEN, H. K. 1978 Heat or mass transfer from an open cavity. *J. Engng Maths* **12**, 129.

KUIKEN, H. K. 1981*a* A backward free-convective boundary layer. *Q. J. Mech. Appl. Maths* **34**, 397.

KUIKEN, H. K. 1981*b* On boundary layers in fluid mechanics that decay algebraically along stretches of wall that are not vanishingly small. *IMA J. Appl. Maths* **27**, 387.

KUIKEN, H. K. & ROTEM, A. 1971 Asymptotic solution for plumes at very large and very small Prandtl numbers. *J. Fluid Mech.* **45**, 585.

LIGHTHILL, M. J. 1950 Contributions to the theory of heat transfer through a laminar boundary layer. *Proc. R. Soc. Lond.* A **202**, 359.

OSTRACH, S. 1982 Low-gravity fluid flows. *Ann. Rev. Fluid Mech.* **14**, 313.

ROBERTS, G. O. 1977 Fast viscous convection. *Geophys. Astrophys. Fluid Dyn.* **8**, 197.

ROBERTS, G. O. 1979 Fast viscous Bénard convection. *Geophys. Astrophys. Fluid Dyn.* **12**, 235.

SEN, A. K. & DAVIS, S. H. 1982 Steady thermocapillary flows in two-dimensional slots. *J. Fluid Mech.* **121**, 163.

SIRIGNANO, W. A. & GLASSMAN, I. 1970 Flame spreading above liquid fuels: surface-tension-driven flows. *Combust. Sci. Tech.* **1**, 307.

TORRANCE, K. E. 1971 Subsurface flows preceding flame spread over a liquid fuel. *Combust. Sci. Tech.* **3**, 133.

WESSELING, P. 1969 Laminar convection cells at high Rayleigh number. *J. Fluid Mech.* **36**, 625.